

**Discrete energy levels of bright solitons in lithium niobate ferroelectrics**Pradipta Giri,<sup>1,2</sup> Kamal Choudhary,<sup>1,3</sup> Arghya Dey,<sup>1</sup> Arindam Biswas,<sup>2</sup> Aniruddha Ghosal,<sup>2</sup> and A. K. Bandyopadhyay<sup>1,\*</sup><sup>1</sup>*Calcutta Institute of Engineering & Management, W. B. University of Technology, 24/1A, C. G. Road, Calcutta 700040, India*<sup>2</sup>*Institute of Radio Physics & Electronics, University of Calcutta, Calcutta, India*<sup>3</sup>*Department of Materials Science & Engineering, University of Florida, Gainesville, Florida 32611, USA*

(Received 14 June 2012; revised manuscript received 25 August 2012; published 1 November 2012)

In the framework of a simple model of a one-dimensional array of a ferroelectric slab of domains, the polarization with time and space is explained by the Klein-Gordon equation. A perturbation of the K-G equation makes it possible to use this continuum model through a progressive-wave nonlinear Schrödinger equation (NLSE). The latter gives rise to a bright soliton that moves with a certain velocity. The bright soliton controls itself so that both bright and dark solitons appear at the same time with discrete energy levels that are estimated from a hypergeometric function, but the dark soliton is not visible as it is part of the complex solution that indicates absorption of energy, i.e., the presence of an energy gap. The pulse width for switching of ferroelectrics can be estimated from the analysis of the NLSE and matches that calculated from this model.

DOI: [10.1103/PhysRevB.86.184101](https://doi.org/10.1103/PhysRevB.86.184101)

PACS number(s): 05.45.Yv, 77.84.-s, 77.80.Dj, 77.80.Fm

**I. INTRODUCTION**

In the field of applied physics, one of the most well studied materials is ferroelectrics, which have a variety of important applications<sup>1-4</sup> in nonlinear optics, such as electro-optics and second-harmonic generation<sup>5,6</sup> and nonvolatile memory devices.<sup>7,8</sup> Ferroelectrics have also emerged as important materials as piezoelectric transducers, pyroelectric detectors, surface acoustic wave (SAW) devices, and four-phase mixing doublers. Both lithium tantalate and lithium niobate appear to be promising candidates as the key photonic materials for a variety of devices, such as optical parametric oscillators, nonlinear frequency converters and second-order nonlinear optical material, and holography. Many such devices include important nanodevices.<sup>9-11</sup>

Ferroelectricity is an electrical phenomenon whereby certain materials exhibit a spontaneous dipole moment whose direction can be switched between the equivalent states by the application of an external electric field.<sup>1-4</sup> It arises in certain crystal systems that undergo second-order structural transition below the Curie temperature, which results in the development of spontaneous polarization. This can be explained by the Landau-Ginzburg free energy functional.<sup>3,4,9</sup> The ferroelectric behavior is commonly explained by the rotation of domains and domain walls that are present in the crystal with uniform polarization.<sup>1-4</sup> This behavior is nonlinear in terms of hysteresis of polarization ( $P$ ) and electric field ( $E$ ) vectors.

Ferroelectricity arises because of the collections of domains, where the ferroelectric domains, as with ferromagnetic domains, are created and oriented by a need to minimize the fields as well as the free energy of the crystal. The bulk properties and domain structure of these materials have been extensively studied.<sup>3,4,9,12-16</sup> However, recently they have gained renewed interest for potential applications in nanoscience and the design of nanodevices, where the focus is on properties exhibited at small length scales.<sup>9,11</sup> Because of these current interests, we look for details of the dynamical properties of domain arrays, which may become significant features at some of the length scales of interest and thus this issue assumes special significance.

Several studies have been made by Vanderbilt *et al.*<sup>17</sup> on the *ab initio* calculation of energy of the domain wall having a narrow width of the order of one lattice spacing as well as on defect pinning of the domain wall in lead titanate.<sup>18</sup> By powerful NMR experiments on intrinsic defects of ferroelectrics, Yatsenko *et al.*<sup>19</sup> did an impressive study on domain dynamics of lithium and antisite niobium defects structure. Phillpot and coworkers<sup>20</sup> used a density functional theory (DFT) approach and molecular dynamics simulations to show that the 180° domain walls have mixed character in lead titanate and lithium niobate that can be dramatically enhanced in nanoscale thin film heterostructures, where the internal wall structure can form polarization vortices. They also showed<sup>21</sup> the behavior of Er defects in lithium niobate by energetic and stability considerations by DFT combined with thermodynamic calculation, which yields exclusively the role of defects on the charge balance.

Quantum chemical calculations were also undertaken by Stashans *et al.*<sup>22</sup> on the oxygen vacancy defects in lead titanate crystals. It should be mentioned that the relaxor ferroelectrics and intrinsic inhomogeneity were also studied by Bussman-Holder *et al.*<sup>23</sup> for a dielectrically soft matrix. The phenomenological level of description has been used in many previous theoretical and experimental investigations of ferroelectric domain walls, particularly by Scott and coworkers.<sup>7,8</sup> First-principles calculations have also been performed on ferroelectrics by Klotins *et al.*<sup>24</sup> in terms of nano polar regions. An interesting investigation on the domain structure by dynamic-contact “electrostatic force microscopy” also revealed that the distribution of polar nanoregions and their dynamics are influenced by the grain morphology, orientation, and more importantly, oxygen vacancies.<sup>25</sup> Some of these investigations have been made to get an overview of the domains and domain walls in such materials in terms of “smaller length scales” in which the excitations can exist.

The above description also shows the importance of the domain wall in ferroelectrics in describing a soliton solution, i.e., nonlinear localized traveling waves that are robust and propagate without change in shape, giving the polarization profile and the distribution of the elastic strain across the

domain wall.<sup>26</sup> As also indicated in Ref. 26, the ferro-para phase change occurs through a global and coordinate displacement of the ions. Hence, the presence of solitons is due to the Landau double well potential in which the pentavalent metal ions (niobium or tantalum) are sitting with their coupling that is strong enough to lead to cooperative effects. A two-well potential of Landau-Ginzburg has been used to derive the kink solution of the nonlinear propagating waves in ferroelectrics in the context of a diatomic chain model.<sup>27-29</sup> The impact of this potential in the case of a discrete system has been quite extensively studied by Comte<sup>30</sup> (see references therein).

Within the continuum limit dynamics, the nonlinear Klein-Gordon (K-G) equation with second-order space and time derivatives has been used in a number of studies on domain walls and the motion of domain walls, and in some preliminary treatments of arrays of domains.<sup>14</sup> A particular facility in the treatment is that the K-G equation is a well-known equation of mathematical physics which exhibits a wide variety of interesting properties and has applications to a wide variety of different physical systems. A set of intrinsic localized modes or discrete breathers (DBs) of the domain array was also investigated in the context of the Klein-Gordon equation.<sup>9</sup> These excitations are characterized by their long-time oscillations and are highly localized pulses in space that are found in the discrete nonlinear model formulation. DBs are discrete solutions, periodic in time and localized in space, and whose frequencies extend outside the phonon spectrum. They are formed as a self-consistent interaction or coupling between the mode and the system nonlinearity. Thus, DBs modify the local properties of the system that provides the environment for the DBs to exist.

Without going into the history of DBs, it can be said that there has been a considerable amount of research activity on DBs since the paper of Sievers and Takeno<sup>31</sup> was published in 1988. An extensive study on the subject was done by Flach and coworkers<sup>32,33</sup> and by Mackay and Aubry<sup>34,35</sup> that was also followed by a lucid presentation on what we know about discrete quantum breathers by Fleurov.<sup>36</sup> Here, a brilliant review by Flach and Gorbach<sup>37</sup> also needs a special mention that contains almost all the relevant references on DBs. It is pertinent to mention that a richer variety of the Klein-Gordon equation was also derived in the case of other important nonlinear optical materials such as split-ring resonator based metamaterials, where a discrete breather pulse has been observed.<sup>38,39</sup> The Fano resonance due to DBs has also been described on a two-channel ansatz in the K-G lattice by various workers.<sup>40-42</sup> Recently, it was shown in terms of various parameters such as dielectric permittivity, coupling, and focusing-defocusing in metamaterials.<sup>43</sup>

Furthermore, as the discreteness is found to trap the breathers, the moving breathers are nonexistent in a highly discrete nonlinear system that has been lucidly presented by Bang and Peyrard in the context of a Klein-Gordon model.<sup>44</sup> Another relevant work by the same authors<sup>45</sup> needs to be mentioned on a numerical study on the “exchange of energy and momentum” between the colliding breathers to describe an effective mechanism of “energy localization” in the Klein-Gordon lattice, arising out of the discreteness and nonintegrability of the system. In the latter work, the bright soliton solutions have been used in the context of

nonlinear dynamics of DNA molecules to demonstrate the generation of highly localized modes. These two references have significance for our present work, as we are primarily concerned with the derivation of the NLSE through the perturbation route for ferroelectrics, wherein localization also plays a role for discrete breathers.<sup>9</sup>

It is known that quasi-phase-matching (QPM) is an important issue in a quadratic nonlinear photonic crystal (QNPC) or photonic band gap materials with tunability. In an interesting work on QPM by Kobayakov *et al.*,<sup>46</sup> the influence of an induced cubic nonlinearity on the amplitude and phase modulation was analytically studied to predict an efficient all-optical switching. Further, in the application front for a QNPC, a stable soliton solution was shown by Corney and Bang<sup>47</sup> for cubic nonlinearity (induced by dual QPM gratings) and QNPC was found to support both dark and bright solitons even in the absence of quadratic nonlinearity. The “modulation instability” in periodic quadratic nonlinear materials was also investigated by the same authors.<sup>48</sup> Trapani *et al.*<sup>49</sup> studied focusing and defocusing nonlinearities in the context of parametric wave mixing.

The literature on solitons is so vast that it is very difficult to mention all the references. However, Ref. 26 is very useful for further references. For soliton propagation, in many optical systems, it is a common practice to use the nonlinear Schrödinger equation (NLSE). Here it is shown that the NLSE can be derived through perturbation on the K-G equation when a progressive wave passes through a nonlinear medium, such as lithium niobate ferroelectrics, where dispersion may take place. It has been observed that a soliton with higher velocity gives rise to a bright soliton and that moving with lower velocity gives rise to dark soliton in the context of a continuum Hamiltonian.<sup>14</sup> This velocity involves an “interaction constant” that is associated with the spatial term, which seems to guide the soliton behavior, i.e., the shape and velocity of soliton propagation in the ferroelectric system, as considered here. A peculiarity is observed in the solution of the NLSE when soliton-soliton coupling is considered. The soliton has discrete energy levels due to dipole-dipole interaction and a hypergeometric function is derived for the ferroelectric system for discrete energy levels of solitons. All these cases are discussed in the realm of stability of domains in the specific case of lithium niobate ferroelectrics. Although the NLSE has been described for a general system and for DNA macromolecules,<sup>44,45</sup> our perturbation analysis is primarily focused on both the dark and bright solitons in the ferroelectric system.

The paper is organized as follows: In Sec. II, theoretical descriptions are given on the perturbation approach on the K-G equation and derivation of the hypergeometric function for discrete energy levels of solitons. In Sec. III, the results and discussion are presented on soliton wave functions and soliton velocity. Section IV gives the conclusions.

## II. THEORETICAL DEVELOPMENT

Let us consider an idealized one-dimensional array of  $N$  identical ferroelectric domains along the  $x$  direction. The domains are considered to be rectangular parallelepipeds. For simplicity, the polarizations in each domain are oriented in

the  $z$  direction and translationally invariant in the  $y$  direction. Between the neighboring domains, there is a domain wall and here we consider nearest-neighbor coupling between the domains. The domain arrangement has been shown in Ref. 9. For the mode dynamics of the extended modes and modes that are localized, the nonlinear Klein-Gordon equation relating the polarization ( $P$ ) vector in terms of space ( $x$ ) and time ( $t$ ) with rms driving field ( $E_0$ ) is given by<sup>14</sup>

$$\frac{\partial^2 P}{\partial t^2} - \bar{K} \frac{\partial^2 P}{\partial x^2} + \bar{\gamma} \frac{\partial P}{\partial t} - \bar{\alpha}_1 P + \bar{\alpha}_2 P^3 - E_0 = 0 \quad (1)$$

for the dynamics of polarization  $P(x,t)$ . Here, Eq. (1) contains all the nondimensional terms as  $P = P'/P_s$ , where  $P_s$  is the saturation polarization in C/m<sup>2</sup> [typical value for LiNbO<sub>3</sub> ferroelectrics as 0.75 C/m<sup>2</sup> (Ref. 3)]; the normalized field is  $E_0 = E'/E_c$ , where  $E_c$  is the coercive field (when  $P = 0$ ) in kV/cm in the usual nonlinear hysteresis curve of  $P$  vs  $E$  with a typical value for the same material as 40 kV/cm;<sup>3</sup>  $t = t'/t_c$ , where  $t_c$  is considered as the critical time scale for polarization to reach a saturation value, i.e., at or near the domain walls that are of importance to our study with a typical value of 10 ns for a switching time of (say) 200 ns for a damping value  $\bar{\gamma} = 0.50$  (Ref. 15) that are based on the above data; and  $x = x'/W_L$ , where  $W_L =$  domain wall width of the order of a few nanometers. Equation (1) is obtained after dropping the prime notation, and by taking  $\alpha_1 = \alpha_2/P_s^2$  and  $\bar{\alpha}_1 = \bar{\alpha}_2 = \bar{\alpha} = (\alpha_1 P_s)/E_c$ .<sup>3,9</sup> Here, the coefficients associated with the variation of the second-order spatial term for an interaction or coupling ( $K$ ) and that for first-order time variation in Eq. (1) for a damping term ( $\gamma$ ) are given by  $\bar{K} = KP_s/2E_c$  and  $\bar{\gamma} = \gamma P_s/t_c E_c$ , where  $\gamma$  is a decay constant relating to the loss of polarization due to internal friction during the rotational motion of the domains in the system.

For a perturbation analysis, if  $\varepsilon$  is a small parameter characterizing the nonlinearity, the solution of Eq. (1) is considered as

$$P = P' + \varepsilon P_0 + \varepsilon^2 P_1 + \varepsilon^3 P_2 + \dots, \quad (2)$$

where  $P' = \sqrt{\bar{\alpha}_1/\bar{\alpha}_2} \approx 1$  (Ref. 9) and  $P_1, P_2, \dots, P_n$  are the perturbed polarizations. Let us introduce the large-scale variables  $X = \varepsilon x$ ,  $T = \varepsilon t$ , and a new term,  $\tau = \varepsilon T = \varepsilon^2 T$ , where small parameter  $\varepsilon$  is constant, as discussed later. It is to be noted that our analysis can even be done without involving the above new term, but we wanted our perturbation method to be more stringent. In our multiple scale analysis  $\frac{\partial}{\partial t}$  is replaced by  $(\frac{\partial}{\partial t} + \varepsilon \frac{\partial}{\partial T})$  and  $\frac{\partial}{\partial x}$  by  $(\frac{\partial}{\partial x} + \varepsilon \frac{\partial}{\partial X})$ . So, in terms of small parameter, both the temporal and spatial terms can be written as

$$\left( \frac{\partial}{\partial t} + \varepsilon \frac{\partial}{\partial T} \right)^2 = \frac{\partial^2}{\partial t^2} + 2\varepsilon \frac{\partial^2}{\partial t \partial T} + \varepsilon^2 \frac{\partial^2}{\partial T^2}, \quad (3a)$$

$$\left( \frac{\partial}{\partial x} + \varepsilon \frac{\partial}{\partial X} \right)^2 = \frac{\partial^2}{\partial x^2} + 2\varepsilon \frac{\partial^2}{\partial x \partial X} + \varepsilon^2 \frac{\partial^2}{\partial X^2}. \quad (3b)$$

Using Eqs. (3a) and (3b), Eq. (1) leads to the choice of the operators such that they are related as

$$L = L^0 + \varepsilon L^1 + \varepsilon^2 L^2 + \dots \quad (3c)$$

The different components of the above operators are then written as

$$L^{(0)} = \frac{\partial^2}{\partial t^2} - \bar{K} \frac{\partial^2}{\partial x^2} + \bar{\gamma} \frac{\partial}{\partial t}, \quad (4a)$$

$$L^{(1)} = 2 \left( \frac{\partial^2}{\partial t \partial T} + \frac{1}{2} \bar{\gamma} \frac{\partial}{\partial T} - \bar{K} \frac{\partial^2}{\partial x \partial X} \right), \quad (4b)$$

$$L^{(2)} = \left( \frac{\partial^2}{\partial T^2} - \frac{\partial^2}{\partial t \partial \tau} - \bar{K} \frac{\partial^2}{\partial X^2} \right), \quad (4c)$$

where  $\tau = \varepsilon T$ .

In this continuum model, the polarized wave propagates in a progressive manner through the ferroelectric slabs in a one-dimensional array of domains that is expressed as

$$P_0 = \psi(X, T) e^{i(kx - \omega t)}. \quad (5)$$

The nonlinearity is manifested through variable amplitude  $\psi(X, T)$  of the material response. Linear frequency ( $\omega$ ) and propagation constant ( $k$ ) are intrinsic properties of unperturbed polarization in ferroelectrics. The use of Eqs. (2) and (3c) in Eq. (1) gives rise to an equation that is independent of the parameter  $\varepsilon^1$  that operates on Eq. (5) such that  $L^0 P_0 = -2\bar{\alpha}_1 P_0$  in the continuum model. Hence, the result is expressed as

$$\begin{aligned} -\omega^2 + \bar{K} k^2 - i\omega\bar{\gamma} + 2\bar{\alpha}_1 &= 0, \quad \text{or} \\ \omega(\omega + i\bar{\gamma}) &= \bar{K} k^2 + 2\bar{\alpha}_1, \quad \text{or} \\ \omega &= \frac{\omega(\bar{K} k^2 + 2\bar{\alpha}_1)}{\omega^2 + \bar{\gamma}^2} - \frac{i\bar{\gamma}(\bar{K} k^2 + 2\bar{\alpha}_1)}{\omega^2 + \bar{\gamma}^2}. \end{aligned} \quad (6)$$

Taking the real parts, the concerned equation gives rise to a relation of frequency with dispersion modes in the ferroelectrics as

$$\omega^2 = \bar{K} k^2 + 2\bar{\alpha}_1 - \bar{\gamma}^2. \quad (7)$$

In an array of domains, the domain wall stands between the two uniform dipoles that are in opposite direction. There are no waves or dispersion frequency at the domain wall. So we adopt the discrete model rather than the continuum case in dispersion as a special case up to Eq. (11). Now, if we use the discrete concept to take care of smaller length scale of excitation, i.e., in the nano range,  $L^0 P_0 = -2\bar{\alpha}_1 P_0$ . At this stage, if we use the discrete polarization modes  $P_n$  for the  $n$ th domain, and only use the unperturbed part to take care of smaller length scales of excitation, Eq. (1) with the help of the operator in Eq. (4a) can be written as

$$\begin{aligned} \frac{\partial^2 P_0}{\partial t^2} - \bar{K} (P_{0(n+1)} + P_{0(n-1)} - 2P_{0n}) + \bar{\gamma} \frac{\partial P_0}{\partial t} \\ + 2\bar{\alpha}_1 P_0 = 0. \end{aligned} \quad (8)$$

Here, it is to be noted that we consider the nearest neighbors of the  $n$ th domain; hence  $P_{n+1}$  and  $P_{n-1}$  are taken into account. The polarization waves maintain the periodicity, and if we take  $a$  as the lattice constant and  $k$  as the propagation constant, then as per the Bloch theorem, we get  $P_{0(n+1)} = P_0 e^{ika}$ ,  $P_{0(n-1)} = P_0 e^{-ika}$ , and  $P_{0n} = P_0$ . Let us use these relations in the above Eq. (8), and for the discrete case for dispersion, we get

$$-\omega^2 + 4\bar{K} \sin^2 \frac{ka}{2} - i\bar{\gamma}\omega + 2\bar{\alpha}_1. \quad (9)$$

As lithium niobates contain a niobium antisite vacancy, we are inclined to attribute the resulting modes to the impurities and nonlinearity,<sup>9</sup> as the presence of quantum breathers has been related to the presence of such impurities in lithium niobates,<sup>50</sup> as also extensively investigated by Phillpot and coworkers by the density functional theory (DFT) approach and phase field modeling.<sup>20,21</sup> The impurity-induced localized mode oscillations are mainly present in the vicinity of the impurity sites. On the other hand, these excitations exist at any point in the ferroelectric domains. In the realm of nano science and technology, the importance of discrete domains in the smaller length scale cannot be denied, and thus the domains could be better understood. The real value of dispersion frequency in ferroelectric medium in discrete domains is given as

$$\omega^2 = 4\bar{K} \sin^2 \frac{ka}{2} - \bar{\gamma}^2 + 2\bar{\alpha}_1 \quad \text{for} \quad \frac{-\pi}{a} \leq k \leq \frac{\pi}{a}. \quad (10)$$

Here, the propagation constant  $k$  lies within the first Brillouin zone. If  $E_0 = 0$  and  $\bar{\gamma}^2$  is very small (i.e., damping tends to zero<sup>14</sup>), then the minimum frequency for dispersion is defined as

$$\omega_{\min} = \sqrt{2\bar{\alpha}_1}, \quad \text{i.e.,} \quad \omega > \omega_{\min}. \quad (11)$$

Now, coming back to the continuum case, by using Eqs. (2) and (3c), the coefficient of the second-order term  $\varepsilon^2$  is  $L^1 P_0 + L^0 P_1 = 0$ . As  $P_1$  is not involved in this analysis, the second term should be considered zero:  $L^0 P_1 = 0$ . So, the first term  $L^1 P_0 = 0$ . This condition evaluates the partial differential equation as

$$2i \left( \omega \frac{\partial \psi}{\partial T} + i \frac{1}{2} \bar{\gamma} \frac{\partial \psi}{\partial T} + \bar{K} k \frac{\partial \psi}{\partial X} \right) = 0,$$

and for the continuum case for an array of ferroelectric domains, we have

$$\frac{\partial \psi}{\partial T} = -v \frac{\partial \psi}{\partial X}, \quad (12)$$

where  $v$  is the group velocity, which cannot be termed as the velocity of the soliton as we arrive at the soliton solution at Eq. (17), and this is defined as  $v = 2\bar{K}k/(2\omega + i\bar{\gamma})$ . The magnitude of this velocity is given by

$$v = \frac{2\bar{K}k}{\sqrt{4\omega^2 + \bar{\gamma}^2}}. \quad (13)$$

This is the group velocity that decreases with increasing damping. In the continuum model, the nonlinearity is linked to this velocity ( $v$ ) and the spatial distance as

$$\xi = X - vT. \quad (14)$$

Hence, we can write

$$\frac{\partial^2 \psi}{\partial T^2} = v^2 \frac{\partial^2 \psi}{\partial \xi^2}. \quad (15)$$

By using Eqs. (2) and (3c), the coefficient of the third-order term  $\varepsilon^3$  is  $L^2 P_0 + \bar{\alpha}_2 P_0^3 = 0$ . By using Eqs. (14) and (15), this condition gives rise to the nonlinear Schrödinger equation (NLSE):

$$i \frac{\partial \psi}{\partial \tau} + \Omega' \frac{\partial^2 \psi}{\partial \xi^2} + \beta |\psi|^2 \psi = 0. \quad (16)$$

Here,  $\bar{\alpha}_1 = \bar{\alpha}_2$ ,  $\Omega' = (v^2 - \bar{K})/\omega$ , and  $\beta = \bar{\alpha}_2/\omega$ . The solution of Eq. (16) is

$$\psi = \sqrt{2} \sec h \sqrt{\frac{\bar{\alpha}_1}{v^2 - \bar{K}}} \xi e^{i(\bar{\alpha}_1/\omega)\tau}. \quad (17)$$

So, for the unperturbed polarization, we can write

$$P_0 = \sqrt{2} \sec h \sqrt{\frac{\bar{\alpha}_1}{v^2 - \bar{K}}} \xi e^{i\{kx - [\omega t - (\bar{\alpha}_1/\omega)\tau]\}}. \quad (18)$$

These unperturbed polarization waves will also propagate through the ferroelectric medium only when

$$\omega t \geq \frac{\bar{\alpha}_1 \tau}{\omega}. \quad (19)$$

In the discrete case, the NLSE, i.e., Eq. (16), is capable of tackling  $x$  and  $t$  if and only if  $\tau = \varepsilon^2 t$  and  $X = \varepsilon x$  where  $\varepsilon$  is an unknown constant that is to be determined. Equation (19) implies that minimum linear frequency  $\omega \geq \sqrt{\varepsilon^2 \bar{\alpha}_1}$ . So, by comparing Eqs. (11) and (19), we get  $\varepsilon = \sqrt{2}$ , and then Eqs. (14) and (16) are modified as

$$\xi = \sqrt{2}(x - vt) \quad (20)$$

and

$$i \frac{\partial \psi}{\partial t} + 2\Omega' \frac{\partial^2 \psi}{\partial \xi^2} + 2\beta |\psi|^2 \psi = 0. \quad (21)$$

In the approximation of discrete domains in the nanoscale region, the above NLSE with an attractive term for ( $\beta = +\beta$ ) or repulsive term for ( $\beta = -\beta$ ) gives rise to a normalized solution of the bright soliton as

$$\psi_1 = \sqrt{2} \sec h \sqrt{\frac{\bar{\alpha}_1}{v^2 - \bar{K}}} \xi e^{i(2\bar{\alpha}_1/\omega)t}. \quad (22)$$

When the soliton moves with velocity  $v < \sqrt{\bar{K}}$ , Eq. (21) gives the dark soliton. The normalized solution for the equation of the dark soliton is written as

$$\psi_2 = \tanh \sqrt{\frac{\bar{\alpha}_1}{\bar{K} - v^2}} \xi e^{i(2\bar{\alpha}_1/\omega)t}. \quad (23)$$

In this case, the bright soliton has the probability density as  $|\psi|^2 = \psi \psi^*$  which is the intensity or amplitude of polarization wave such that

$$\psi \psi^* = 2 \sec h^2 \frac{\xi}{\sigma}, \quad (24)$$

where  $\sigma = \sqrt{\frac{v^2 - \bar{K}}{\bar{\alpha}_1}}$ .

A plot of  $\psi^2$  vs  $x$  and  $t$  (not shown here) would show the behavior of the amplitude in the space-time perspective. Now, if we take it as an eigenvalue problem, then let us consider the expression as

$$i \frac{\partial \psi}{\partial t} = E_n \psi. \quad (25)$$

The solitary state exists due to the dipole-dipole interaction in a domain which can be tuned or rather tailored in various ways in the experiment. So, let  $E_n$  be the discrete energy level of

the soliton, then Eq. (21) becomes

$$E_n \psi + 2\Omega' \frac{\partial^2 \psi}{\partial \xi^2} + 4\beta \sec h^2 \frac{\xi}{\sigma} = 0. \quad (26)$$

For the determination of discrete energy levels, let us do a transformation of variables as

$$z = -\sinh^2 \frac{\xi}{\sigma}. \quad (27)$$

Using this transformation of variables, Eq. (26) becomes

$$z(z-1) \frac{d^2 \psi}{dz^2} - \frac{1}{2}(1-2z) \frac{d\psi}{dz} + \left( \frac{\sigma^2 E_n}{8\Omega'} + \frac{2\beta\sigma^2}{4\Omega' \cosh^2 \frac{\xi}{\sigma}} \right) \psi = 0. \quad (28)$$

Let us take a solution of the above equation as

$$\psi = (1-z)^{(\gamma-1)/2} w(z), \quad (29)$$

where an energy term is defined as  $\gamma = 0, 3$  and  $w(z)$  is the ‘‘hypergeometric’’ function. This function is specifically suitable to find the discrete energy levels in lithium niobate ferroelectrics for a study of switching behavior that are useful for applications. By using Eqs. (28) and (29) becomes

$$z(1-z) \frac{d^2 w(z)}{dz^2} + \left( \frac{1}{2} - \gamma z \right) \frac{dw(z)}{dz} + \left( \delta^2 - \frac{(\gamma-1)(\gamma-2)}{4(1-z)} + \frac{(\gamma-1)(\gamma-3)z}{4(1-z)} - \frac{(1-2z)(\gamma-1)}{4(1-z)} \right) w(z) = 0, \quad (30)$$

where  $\delta^2 = -\sigma^2 E/8\Omega'$  is considered in the above equation, and we get

$$z(1-z) \frac{d^2 w(z)}{dz^2} + \left( \frac{1}{2} - \gamma z \right) \frac{dw(z)}{dz} + \left( \delta^2 - \frac{(\gamma-1)^2}{4} \right) w(z) = 0, \quad (31)$$

where  $-a = \delta - (\gamma-1)/2$ ,  $-b = -\delta - (\gamma-1)/2$ , then  $a + b + 1 = \gamma$  and  $(-a)(-b) = \delta^2 - [(1-\gamma)/2]^2$ . Here,  $a$  and  $b$  are integers or fractions. Hence by putting  $\delta - (\gamma-1)/2 = -n/2$ , for  $n = 0, 1, 2, 3, \dots$ , the discrete energy for the bright-soliton motion can be expressed as

$$E_n = -\frac{2\bar{\alpha}_1}{\omega} (n+1)^2 \quad \text{for } \gamma = 0 \quad (32)$$

and

$$E_n = -\frac{2\bar{\alpha}_1}{\omega} (2-n)^2 \quad \text{for } \gamma = 3. \quad (33)$$

The solution of the above Eq. (31) can be written as

$$w(z) = \sum_{r=0}^{\infty} a_r z^{k+r}. \quad (34)$$

The ‘‘series’’ solution can be expressed as

$$w(z) = AF\left(-a, -b, \frac{1}{2}, z\right) + Bz^{1/2} F\left(-a + \frac{1}{2}, -b + \frac{1}{2}, \frac{3}{2}, z\right). \quad (35)$$

Let us discuss some cases with different parameter values:

*Case 1.* When  $k = 0$  and  $r = 0$ . Thus,  $w(z) = a_0$ .

*Case 2.* When  $k = \frac{1}{2}$  and  $r = 0$ . Thus,  $w(z) = a_0 z^{1/2}$ . So,  $w(z) = a_0(1+z^{1/2})$ .

Both spatially variable and time-approximate solution of Eq. (26) is given as

$$\psi(\xi, t) = (1-z)^{(\gamma-1)/2} w(z) = a_0 \left( \sec h \frac{\xi}{\sigma} + i \tanh \frac{\xi}{\sigma} \right) \times \exp \left[ i \frac{2\bar{\alpha}_1 (n+1)^2}{\omega} t \right] \quad \text{for } \gamma = 0, \quad (36)$$

$$\psi(\xi, t) = a_0 \left( \cosh^2 \frac{\xi}{\sigma} + i \cosh^3 \frac{\xi}{\sigma} \right) \times \exp \left[ i \frac{2\bar{\alpha}_1 (2-n)^2}{\omega} t \right] \quad \text{for } \gamma = 3. \quad (37)$$

These two equations have quite an importance, as discussed below. Next, let us do our analysis for a widely used material such as LiNbO<sub>3</sub>, based on the above deductions of NLSE and the hypergeometric function for estimation of the discrete energy levels.

### III. RESULTS AND DISCUSSION

By giving an appropriate perturbation, an analysis of the K-G equation gives rise to the nonlinear Schrödinger equation (NLSE) that is considered in the context of soliton waves, i.e., the second-order linear operators which describe the dispersion and diffraction of the wave packet and nonlinearity. The analysis of the NLSE facilitates the determination of the pulse width for switching of ferroelectrics that are highly congruent, such as lithium tantalates, wherein voluminous work was done by Gopalan and coworkers.<sup>6,51</sup> For optical communication devices, when a wave packet passes through ferroelectric materials, the dispersion would take place near the domain wall and in the absence of dispersion, the soliton will appear near the domain wall.

As lithium niobate contains a niobium antisite vacancy, we are inclined to attribute the resulting modes to the impurities,<sup>9</sup> as the presence of quantum breathers has also been related to the presence of such impurities in lithium niobate.<sup>50</sup> Our K-G equation [Eq. (1)] is derived from our discrete Hamiltonian<sup>9,13</sup> that contains a nondimensional driving field term which involves the poling field ( $E_c$ ). This ‘‘poling field’’ in turn depends on the impurity content, as detailed by Yan *et al.*<sup>52</sup> with an impressive set of data on lithium niobates, while modeling the domain structure. Thus, our Hamiltonian is impurity dependent.<sup>9</sup> Also, the presence of charged defects has been extensively investigated by Phillpot and coworkers by density functional theory (DFT) approach and phase field modeling<sup>20,21</sup> for Er defects in ferroelectrics. The impurity-induced localized mode oscillations are mainly present in the vicinity of the impurity sites. On the other hand, these

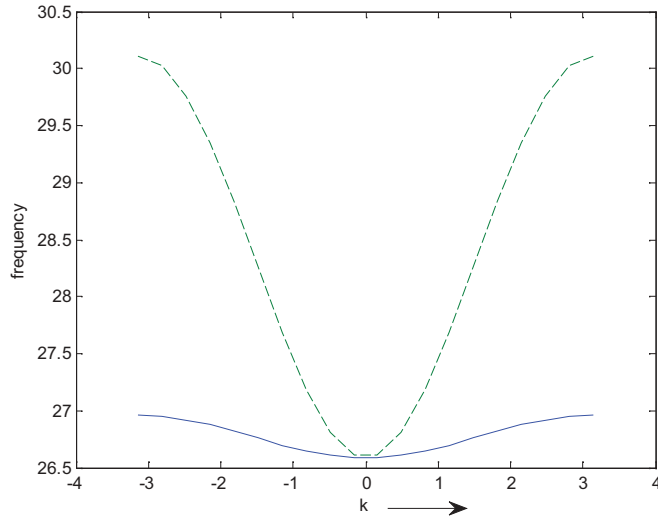


FIG. 1. (Color online) The dashed line is the curve for  $\bar{K} = 100$  and the solid line for  $\bar{K} = 10$ .

excitations exist at any point in the ferroelectric domains. As the importance of discrete domains in the smaller length scale cannot be denied, the real value of dispersion frequency<sup>53</sup> in ferroelectric medium in discrete domains is given by Eq. (11) for zero driving field and low damping value.

As per Eq. (10), for two different values of  $\bar{K}$ , for positive pulse in the switch-on state, a plot of frequency vs propagation constant is shown in Fig. 1. Normally, the higher coupling has higher slope ( $d\omega/dk$ ) that gives rise to higher dispersion. It is seen that at lower values of interaction constant, the minimum is hardly discernible at zero wave number, whereas a very high value of coupling in the system gives rise to a distinct minimum to show the effect of increasing coupling. The linear frequency [as per Eq. (11)] is  $\omega > \sqrt{2\bar{\alpha}_1}$ , as discussed before. By the above mathematical analysis, it is observed that pulse width is 0.12 sec or 120 ms. This corresponds to  $\omega_{\min} = 26.58$  for  $\bar{\alpha}_1 = 353.42$  that is related to an impurity content of 0.133 mole % of niobium antisite charge defects (equivalent to a poling field of 40 kV/cm) with short voltage excitation in the lithium niobate as a result of domain wall motion during forward poling. For lithium tantalite  $\bar{\alpha}_1 = 512.66$  and  $\omega_{\min} = 32.02$ . So, numerically speaking, the required pulse width is  $\approx 0.10$  sec or 100 ms for lithium tantalate, whereas experimentally, the domain wall motion is observed with the use of a Nomarski light microscope during forward poling for pulse width to be 150 ms at a very high value of poling field of 221 kV/cm.<sup>54</sup>

As per Eq. (22), the (bright) solitonic wave function is shown in Fig. 2. The calculations show that the coefficient  $\bar{K}$  involving the dipolar interaction term is very important in contributing to the “soliton motion” in our ferroelectric system, i.e., in terms of its influence on the shape of the solitons with stationary velocity.<sup>14</sup> This interaction constant ( $\bar{K}$ ) is proportional to the square of the domain dimension.<sup>13</sup> When soliton velocity is  $> \bar{K}$ , i.e., the soliton moves faster, it is called a bright soliton<sup>26</sup> that resides in the vicinity of the defect and also at the domain walls. Here,  $\psi_1$  is normalized in the region  $-1.1 \geq \xi \geq 1.1$  when  $v^2 = 4\bar{\alpha}_1 + \bar{K}$ . Under this condition for  $\bar{K} = 10$  and  $\bar{\alpha}_1 = 353.42$ , the typical velocity of the bright

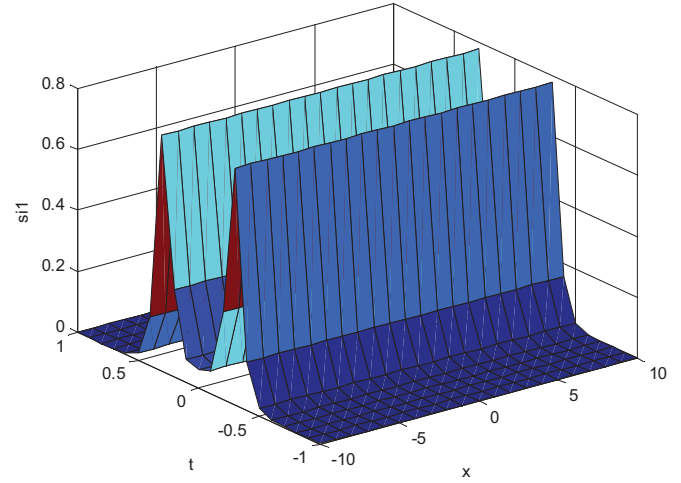


FIG. 2. (Color online) The spatiotemporal behavior of bright-soliton propagation.

soliton will be approximately 37.73 m/sec in lithium niobate. For  $\bar{K} = 100$ , the typical velocity of the bright soliton becomes 38.91 m/sec.

As per Eq. (23), the (dark) solitonic wave function is shown in Fig. 3. It is normalized in the region  $-0.7 \geq \xi \geq 0.7$  when  $v^2 = \bar{K} - \bar{\alpha}_1/36$ . The typical velocity of a dark soliton in lithium niobate is approximately 0.43 m/sec for  $\bar{K} = 10$  and for  $\bar{K} = 100$  that for a dark soliton,  $v = \sqrt{100 - \bar{\alpha}_1}/4 = 3.41$  m/sec. So, the velocity of a dark soliton is very low compared to that of a bright soliton in lithium niobate ferroelectrics, as expected. No relation has been worked out between the soliton velocity and domain wall motion, which can be taken up in our future scope of work. However, it is pertinent to mention one important investigation on a lead-zirconate-titanate with strontium-ruthenium by Kim *et al.*<sup>55</sup> who showed the domain wall velocity to be 0.1–0.5 m/sec. They also related different switching behavior to local field deviation due to dipolar defects. Here, we have also shown that dipole-dipole interaction prevails in our system that is normally enhanced by defects.<sup>9,11</sup> Now, we can write

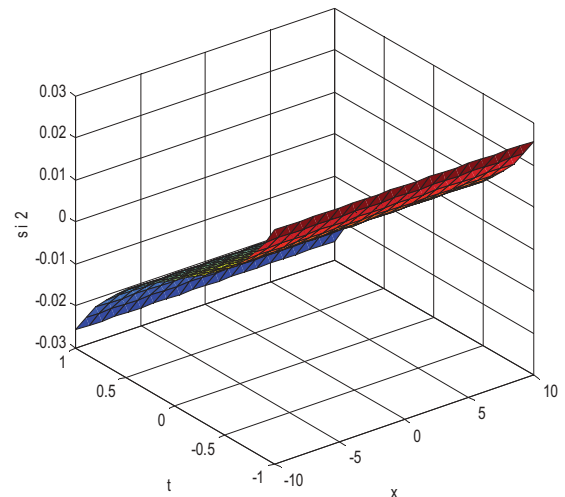


FIG. 3. (Color online) The spatiotemporal behavior of dark-soliton propagation.

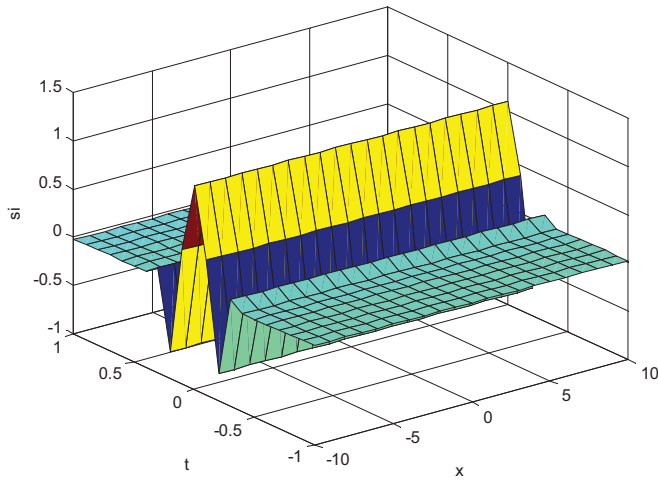


FIG. 4. (Color online) The wave function behavior of Eq. (38), which is the resulting normalized solution of Eq. (21).

the resulting normalized solution of Eq. (21) as

$$\psi = \left( \sqrt{2} \sec h \sqrt{\frac{\bar{\alpha}_1}{v^2 - \bar{K}}} \xi + \tanh \sqrt{\frac{\bar{\alpha}_1}{\bar{K} - v^2}} \xi \right) e^{i(2\bar{\alpha}_1/\omega)t}. \quad (38)$$

When  $v = \sqrt{\bar{K}}$ , only sinusoidal waves propagate through lithium niobate due to relatively lower existence of dark solitons. This is shown in Fig. 4. It is observed that for an interaction between the solitons in highly nonlocal nonlinear media, and for  $\beta = +\beta$ , the solitons are propagating in different parts of the sample. They exhibit properties normally associated with polarization and have a tendency to conserve quantities such as power and momentum, which has an implication for the application in devices. An interaction between the solitons themselves can establish a certain minimal distance between the pulses and hence they can be separated from each other by domain wall width (DWW); i.e., it is thought that a pulse active on a given polarization direction will be separated by a finite distance barrier (DWW) wherein it gets inverted after switching, i.e., when polarization goes to the opposite direction.

Here, the two values of  $\gamma$  (0 and 3) need some explanation. In Eq. (29),  $\gamma = \frac{3}{2} \pm \frac{1}{2} \sqrt{8\beta\sigma^2/\Omega' + 1} = \frac{3}{2} \pm \frac{3}{2}$ . So  $\gamma$  has values 0 or 3 and as detailed in Sec. II, under this condition, only the hypergeometric function is valid. Dark solitons are energetically weaker than bright solitons. When  $v = \bar{K}$  progressive wave packets exist for a finite value of dark solitons, as discussed before.

In terms of discrete energy levels, some explanation needs to be given here. The soliton appears near the domain wall due to interaction between the dipoles. Impurities are also gathered at the domain wall and the steepness of the domain wall is enhanced by the bright soliton along with the low-energetic dark soliton. It is interesting to note that dark solitons always exist [see Eqs. (22) and (38)] even when the bright soliton propagates through the medium with its self-energy that is defined by  $2 \sec h^2 \frac{\xi}{\sigma}$ . So, bright solitons have a certain number of energy levels that depend on the internal obstacle, i.e., damping in the system. There is no obstacle in a region that

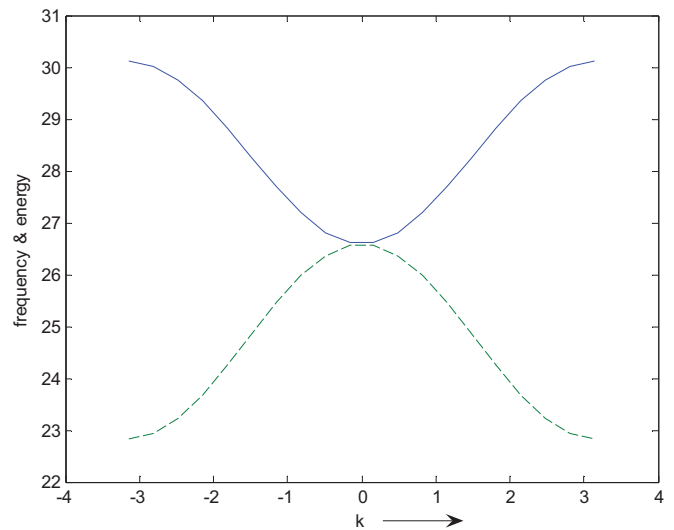


FIG. 5. (Color online) Dispersion is shown by solid line that is maximum at  $-\pi/a$  and  $\pi/a$ ; the dashed line is meant for zero-point energy for this model.

is characterized as an “energy gap” where the dipoles can be rotated by forward and reverse poling. The corresponding domain walls are relatively steeper for forward poling than for reverse poling thus establishing the existence of energy levels of the soliton.<sup>54,56</sup> The condition for unperturbed propagation of waves through the crystal is primarily temperature and impurity dependent for a particular frequency, as deduced from Eq. (19).

Finally, it is important to mention that Eqs. (36) and (37) are quite significant in that if we start with the bright soliton at or near the domain wall in a given ferroelectric, then the solution of the NLSE [Eq. (26)] gives rise to both a real term that is driving the bright soliton in the system and a complex term, i.e., a significant absorption of “energy” that implies a certain band gap, where dark solitons would cease to propagate in the system. When a wave packet passes through lithium niobate ferroelectrics, the dispersion will take place near the domain wall and when dispersion will not exist, the soliton will appear near the domain wall, as shown in Fig. 5. When the bright soliton passes through the self-energy barrier, it splits into real and imaginary parts which are bright and dark solitons, respectively, with discrete energy levels.

#### IV. CONCLUSION

An analysis of the K-G equation gives rise to the nonlinear Schrödinger equation (NLSE) on perturbation that is considered in the context of soliton waves, i.e., the second-order linear operator which describes the dispersion and diffraction of the wave packet and nonlinearity. The validity of the NLSE breaks down near collapse where the assumption of small amplitude and large scale of modulation no longer holds. The effects of perturbations that can modify or even arrest the collapse are also considered. These include dissipation, normal dispersion, and saturated nonlinearity. Both bright and dark solitons are the solutions of NLSE under the conditions  $v > \sqrt{\bar{K}}$  and  $v < \sqrt{\bar{K}}$ , respectively. The bright soliton moves with a velocity of 37.73 m/sec and the dark soliton moves

with a velocity of 0.43 m/sec for  $\bar{K} = 10$ . The soliton has self-energy or amplitude defined as  $2 \text{ sec } h^2 \frac{\xi}{\sigma}$ , and this has an important role in controlling the bright soliton so that the bright soliton has discrete energy levels. When the wave packet passes through lithium niobate ferroelectrics, the dispersion will take place near the domain wall and in the absence of dispersion, the soliton will appear near the domain wall. When the bright soliton passes through the self-energy barrier, it splits into real

and imaginary parts, i.e., bright and dark solitons, respectively, with discrete energy levels.

#### ACKNOWLEDGMENT

The authors would like to thank Jesús Cuevas of the nonlinearity group of the University of Seville (Spain) for many helpful discussions.

\*asisbanerjee1000@gmail.com

- <sup>1</sup>H. Fu and R. E. Cohen, *Nature (London)* **403**, 281 (2000).
- <sup>2</sup>M. E. Lines and A. M. Glass, *Principles and Applications of Ferroelectrics and Related Materials* (Clarendon, Oxford, 1977).
- <sup>3</sup>S. Kim, V. Gopalan, and A. Gruverman, *Appl. Phys. Lett.* **80**, 2740 (2002).
- <sup>4</sup>A. K. Bandyopadhyay and P. C. Ray, *J. Appl. Phys.* **95**, 226 (2004).
- <sup>5</sup>K. T. Gahagan *et al.*, *Appl. Opt.* **38**, 1186 (1999).
- <sup>6</sup>S. Kim, V. Gopalan, K. Kitamura, and Y. Furukawa, *J. Appl. Phys.* **90**, 2949 (2001).
- <sup>7</sup>M. Dawber, K. M. Rabe, and J. F. Scott, *Rev. Mod. Phys.* **77**, 1083 (2005).
- <sup>8</sup>G. Catalan, A. Schilling, J. F. Scott, and J. M. Greg, *J. Phys.: Condens. Matter* **19**, 132201 (2007).
- <sup>9</sup>A. K. Bandyopadhyay, P. C. Ray, L. Vu-Quoc, and A. R. McGurn, *Phys. Rev. B* **81**, 064104 (2010).
- <sup>10</sup>*Nanoelectronics and Information Technology*, edited by R. Waser (Wiley, Weinheim, 2005).
- <sup>11</sup>P. Giri, S. Ghosh, K. Choudhary, Md. Alam, A. K. Bandyopadhyay, and P. C. Ray, *Phys. Scr.* **83**, 015702 (2011).
- <sup>12</sup>V. Srinivas and L. Vu-Quoc, *Ferroelectrics* **163**, 29 (1995).
- <sup>13</sup>A. K. Bandyopadhyay, P. C. Ray, and V. Gopalan, *J. Phys.: Condens. Matter* **18**, 4093 (2006).
- <sup>14</sup>A. K. Bandyopadhyay, P. C. Ray, and V. Gopalan, *Euro. Phys. J. B* **65**, 525 (2008).
- <sup>15</sup>A. K. Bandyopadhyay, P. C. Ray, and V. Gopalan, *J. Appl. Phys.* **100**, 114106 (2006).
- <sup>16</sup>D. A. Scrymgeour, V. Gopalan, A. Itagi, A. Saxena, and P. J. Swart, *Phys. Rev. B* **71**, 184110 (2005).
- <sup>17</sup>B. Meyer and D. Vanderbilt, *Phys. Rev. B* **65**, 104111 (2002).
- <sup>18</sup>L. He and D. Vanderbilt, *Phys. Rev. B* **68**, 134103 (2003).
- <sup>19</sup>A. V. Yatsenko, M. H. Ivanova-Maksikova, and N. A. Sergeev, *Physica B* **254**, 256 (1998).
- <sup>20</sup>D. Lee, R. K. Behera, P. Wu, H. Xu, Y. L. Li, S. B. Sinnott, S. R. Phillpot, L. Q. Chen, and V. Gopalan, *Phys. Rev. B* **80**, 060102 (2009).
- <sup>21</sup>H. Xu, D. Lee, S. B. Sinnott, V. Gopalan, V. Dierolf, and S. R. Phillpot, *Phys. Rev. B* **80**, 144104 (2009).
- <sup>22</sup>A. Stashans, S. Serrano, and P. Medina, *Physica B* **296**, 210 (2001).
- <sup>23</sup>A. Bussmann-Holder, A. R. Bishop, and T. Egami, *Europhys. Lett.* **71**, 249 (2000).
- <sup>24</sup>E. Klotins, *Physica E* **429**, 614 (2010).
- <sup>25</sup>N. S. John, D. Saranya, J. Parui, and S. B. Krupanidhi, *J. Phys. D: Appl. Phys.* **44**, 415401 (2011).
- <sup>26</sup>T. Dauxois and M. Peyrard, *Physics of Solitons* (Cambridge University Press, Cambridge, 2006), p. 211.
- <sup>27</sup>J. A. Gonzalez, L. E. Guerrero, and A. Bellorin, *Phys. Rev. E* **54**, 1265 (1996).
- <sup>28</sup>J. A. Holyst, *Phys. Rev. E* **57**, 4786 (1998).
- <sup>29</sup>G. Benedek, A. Bussmann-Holder, and H. B. Bilz, *Phys. Rev. B* **36**, 630 (1987).
- <sup>30</sup>J. C. Comte, *Phys. Rev. E* **65**, 046619 (2002).
- <sup>31</sup>A. J. Sievers and S. Takeno, *Phys. Rev. Lett.* **61**, 970 (1988).
- <sup>32</sup>S. Flach, *Phys. Rev. E* **51**, 1503 (1995).
- <sup>33</sup>S. Flach and C. R. Willis, *Phys. Rep.* **295**, 181 (1998).
- <sup>34</sup>R. S. Mackay and S. Aubry, *Nonlinearity* **7**, 1623 (1994).
- <sup>35</sup>S. Aubry, *Physica D* **103**, 201 (1997).
- <sup>36</sup>V. Fleurov, *Chaos* **13**, 676 (2003).
- <sup>37</sup>S. Flach and A. V. Gorbach, *Phys. Rep.* **467**, 1 (2008).
- <sup>38</sup>P. Giri, K. Choudhary, A. S. Gupta, A. K. Bandyopadhyay, and A. R. McGurn, *Phys. Rev. B* **84**, 155429 (2011).
- <sup>39</sup>B. Mandal, S. Adhikari, R. Basu, K. Choudhary, S. J. Mandal, A. Biswas, A. K. Bandyopadhyay, A. K. Bhattacharjee, and D. Mandal, *Phys. Scr.* **86**, 015601 (2012).
- <sup>40</sup>S. Flach, A. E. Miroshnichenko, V. Fleurov, and M. V. Fistul, *Phys. Rev. Lett.* **90**, 084101 (2003).
- <sup>41</sup>A. E. Miroshnichenko, S. Flach, and Y. S. Kivshar, *Rev. Mod. Phys.* **82**, 2257 (2010).
- <sup>42</sup>S. W. Kim and S. Kim, *Phys. Rev. B* **63**, 212301 (2001).
- <sup>43</sup>K. Choudhary, S. Adhikari, A. Biswas, A. Ghosal, and A. K. Bandyopadhyay, *J. Opt. Soc. Am. B* **29**, 2414 (2012).
- <sup>44</sup>O. Bang and M. Peyrard, *Physica D* **81**, 9 (1995).
- <sup>45</sup>O. Bang and M. Peyrard, *Phys. Rev. E* **53**, 4143 (1996).
- <sup>46</sup>J. F. Corney and O. Bang, *Phys. Rev. E* **64**, 047601 (2001).
- <sup>47</sup>A. Kobayakov, F. Lederer, O. Bang, and Y. S. Kivshar, *Opt. Lett.* **23**, 506 (1998).
- <sup>48</sup>J. F. Corney and O. Bang, *Phys. Rev. Lett.* **87**, 133901 (2001).
- <sup>49</sup>P. Di Trapani, A. Bramati, S. Minardi, W. Chinaglia, C. Conti, S. Trillo, J. Kilius, and G. Valiulis, *Phys. Rev. Lett.* **87**, 183902 (2001).
- <sup>50</sup>A. Biswas, K. Choudhary, A. K. Bandyopadhyay, A. K. Bhattacharjee, and D. Mandal, *J. Appl. Phys.* **110**, 024104 (2011).
- <sup>51</sup>L. Tian, V. Gopalan, and L. Galambos, *Appl. Phys. Lett.* **85**, 4445 (2004).
- <sup>52</sup>W. Yan, Y. Kong, L. Shi, L. Sun, H. Liu, X. Li, Di Zhao, J. Xu, S. Chen, L. Zhang, Z. Huang, S. Liu, and G. Zhang, *J. Phys. D: Appl. Phys.* **39**, 21 (2006).
- <sup>53</sup>K. Yoshimura and S. Watanabe, *J. Phys. Soc. Jpn.* **60**, 82 (1991).
- <sup>54</sup>V. Gopalan and T. E. Mitchel, *J. Appl. Phys.* **83**, 941 (1998).
- <sup>55</sup>D. J. Kim, J. Y. Jo, Y. S. Kim, and K. S. Song, *J. Phys. D: Appl. Phys.* **43**, 395403 (2010).
- <sup>56</sup>V. Gopalan, *Annu. Rev. Mater. Res.* **37**, 449 (2007).